

Supporting Information for “On the cause of enhanced landward motion of the overriding plate after a major subduction earthquake”

M. D’Acquisto¹, M. W. Herman², R. E. M. Riva³, R. Govers¹

¹Department of Earth Sciences, Utrecht University, Utrecht, the Netherlands

²Department of Geological Sciences, California State University, Bakersfield, USA

³Department of Geoscience & Remote Sensing, Delft University of Technology, Delft, the Netherlands

Contents of this file

1. Figures S1 to S6

Introduction

This supporting information includes additional details of the model results presented in Section 3 (Result and analysis). In particular, it consists of text and figures that briefly describe the quantitative effect of varying model parameters in both the 2D conceptual and 3D seismic cycle models. It complements Sections 3.2 and 3.3, providing numbers and figures that would otherwise clutter the exposition of the results.

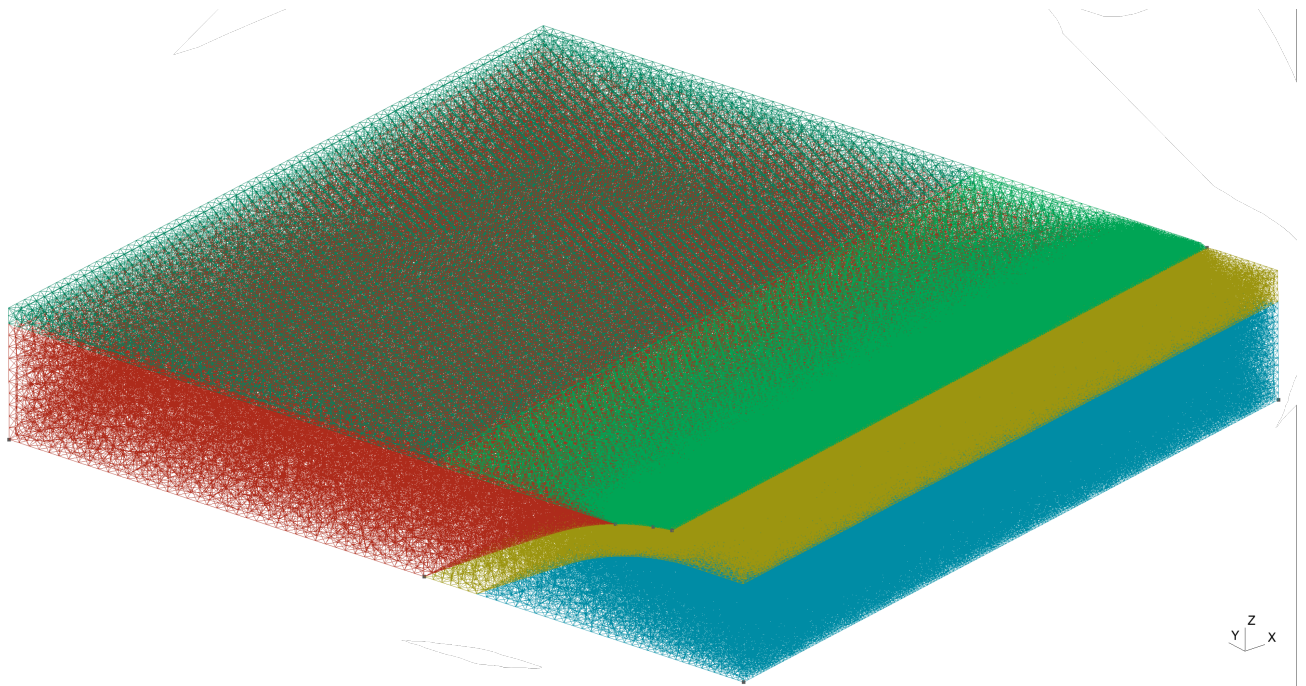


Figure S1. Isometric projection of the finite element mesh used in the reference model (Ref).

Figure S2. Trench-perpendicular surface velocity change 1 year after the earthquake along trench-parallel profiles in the reference model (Ref) at different distances from the trench.

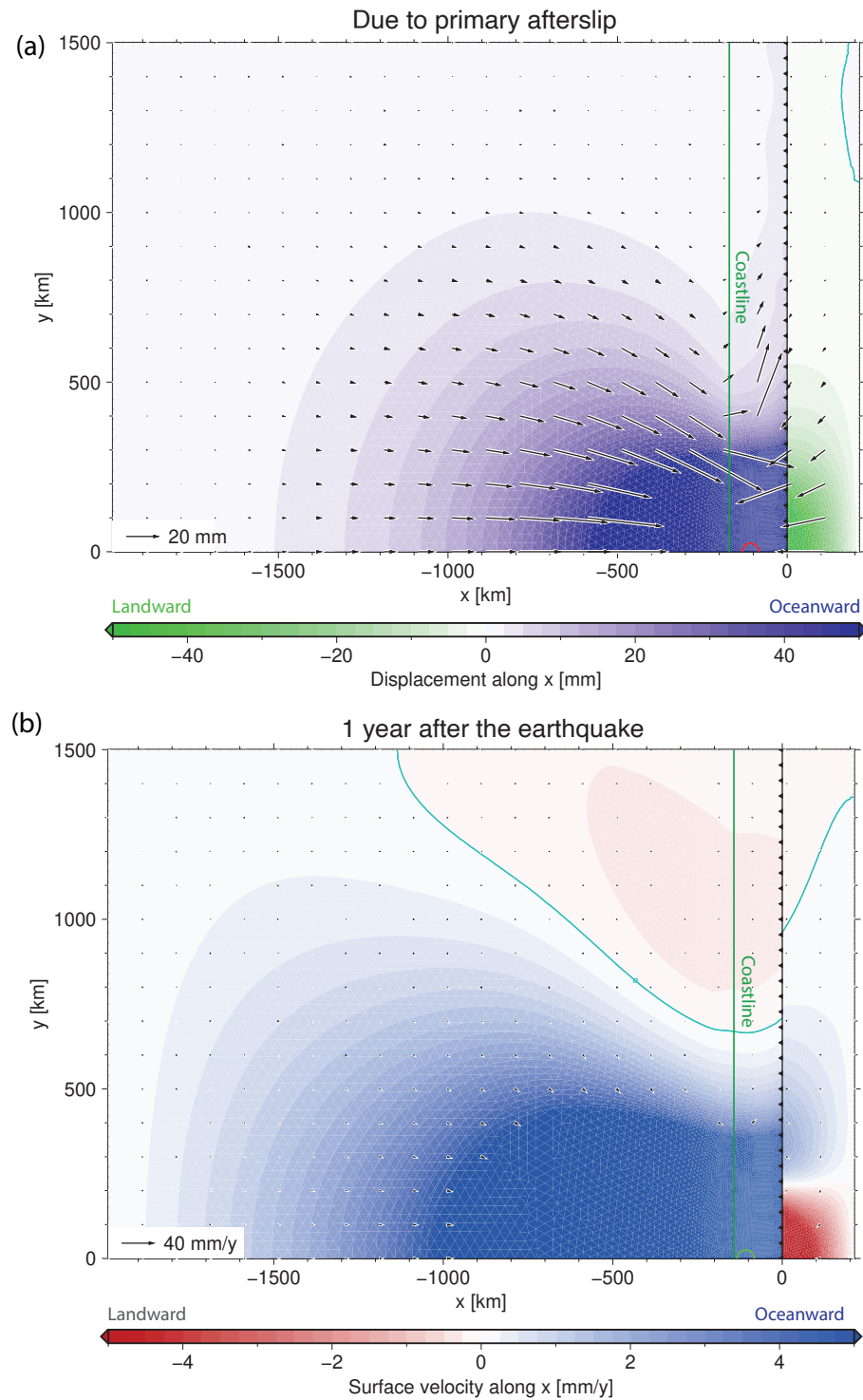


Figure S3. Landward motion due to postseismic relaxation in a model with no time-variable relative motion (afterslip or interseismic slip deficit accumulation) between the slab and mantle at depths greater than 45 km. (a) Displacement due to afterslip. (b) Velocity changes, 1 year after the earthquake, due to viscous relaxation.

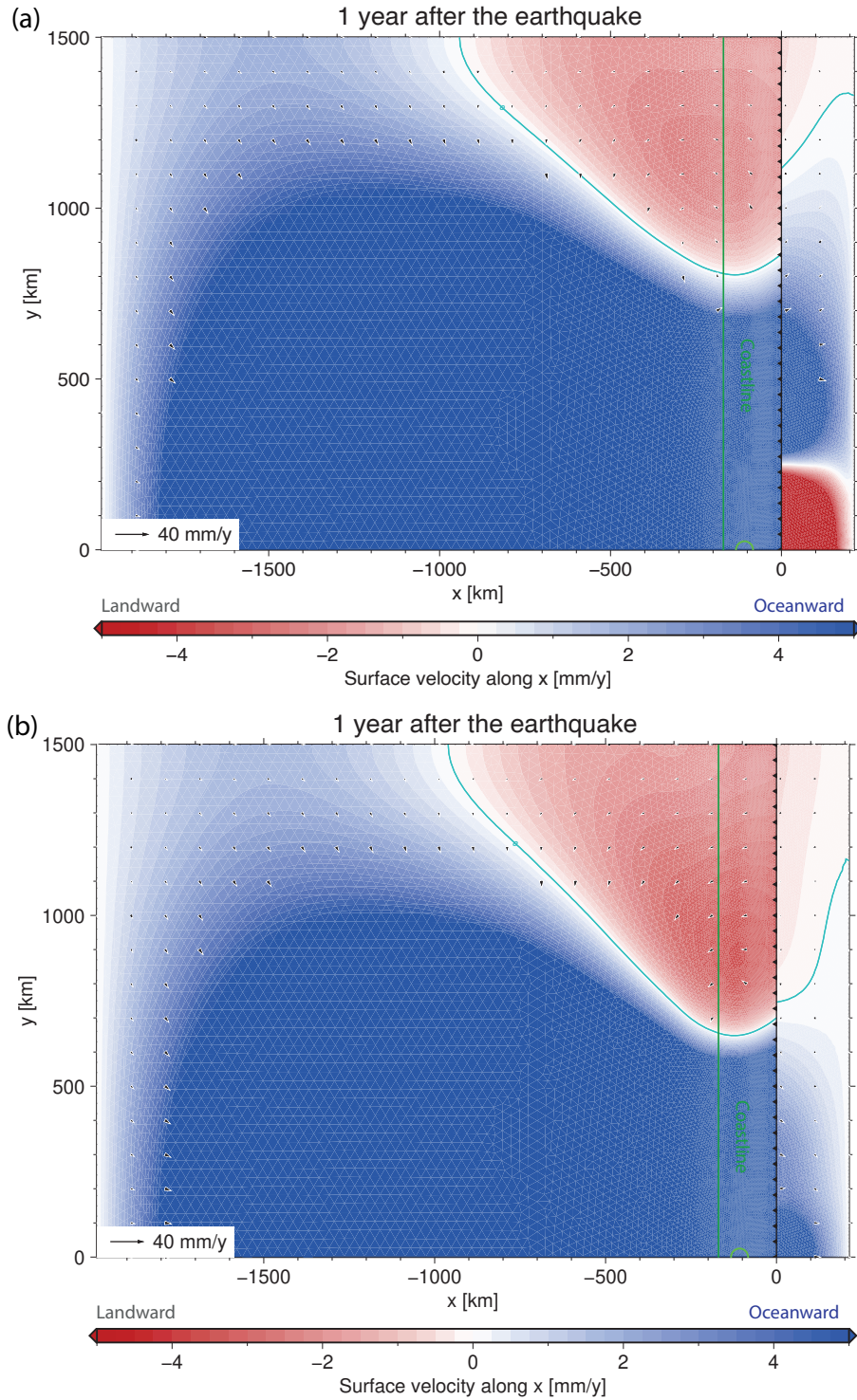


Figure S4. Trench-perpendicular velocity changes $\Delta v_{x1\text{yr-pre}}$, 1 year after the earthquake, due to viscous relaxation, in models with a viscosity of $2 \cdot 10^{18} \text{ Pa} \cdot \text{s}$ in the visco-elastic mantle in (a) both mantle domains (model LoEta1), May 19, 2022 at 7:40 pm, and (b) only in the mantle wedge (model LoEta2). In (b), the sub-slab asthenospheric mantle has the same viscosity ($10^{19} \text{ Pa} \cdot \text{s}$) as both mantle domains in the reference model.

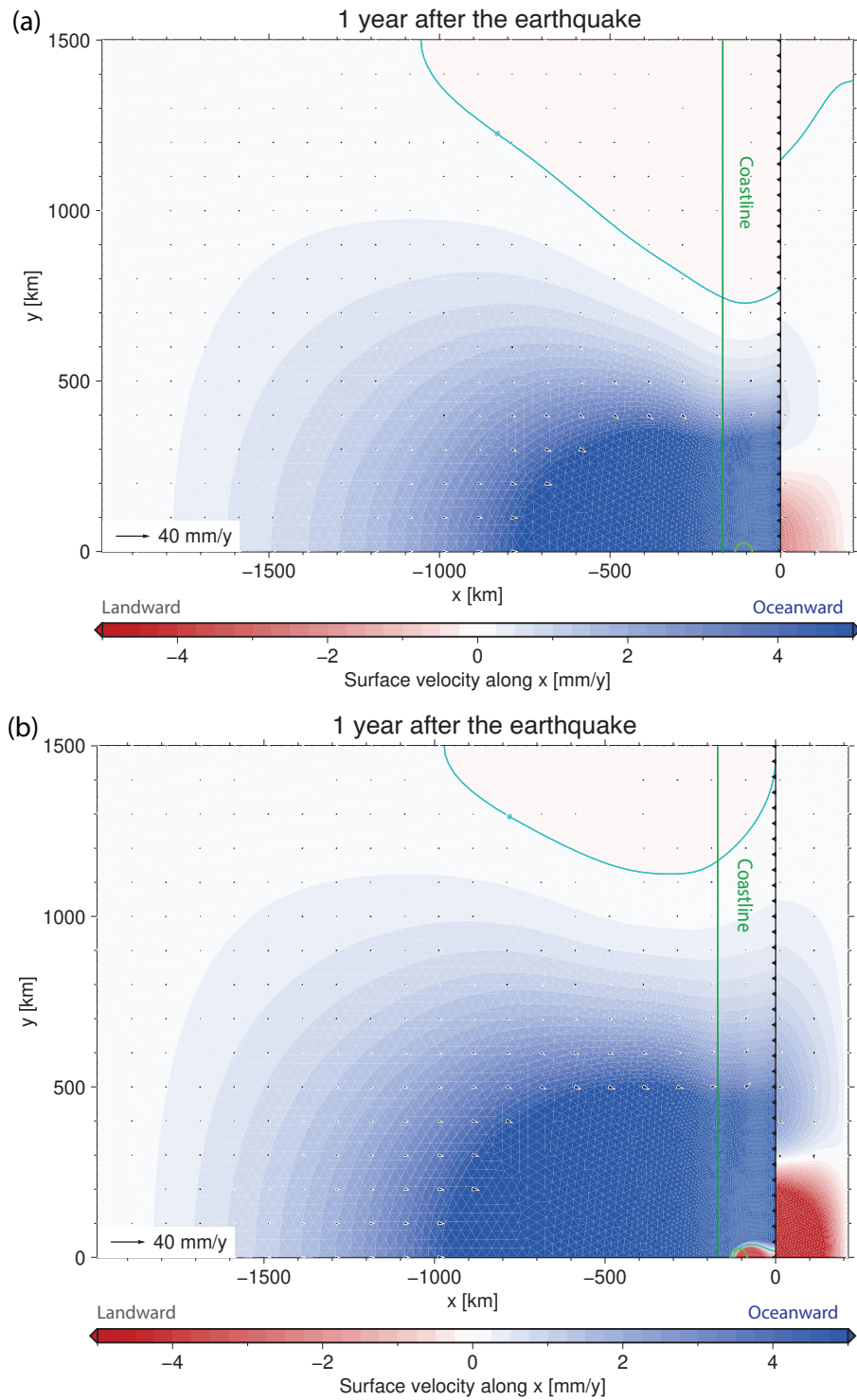


Figure S5. Trench-perpendicular velocity changes $\Delta v_{x1\text{yr-pre}}$, 1 year after the earthquake, due to viscous relaxation, in models with a viscosity of $5 \cdot 10^{19}$ Pa \cdot s in the visco-elastic mantle in (a) both mantle domains (model LoEta1), or (b) only in the mantle wedge (model LoEta2). In (b), the sub-slab asthenospheric mantle has the same viscosity (10^{19} Pa \cdot s) as both mantle domains in the reference model.

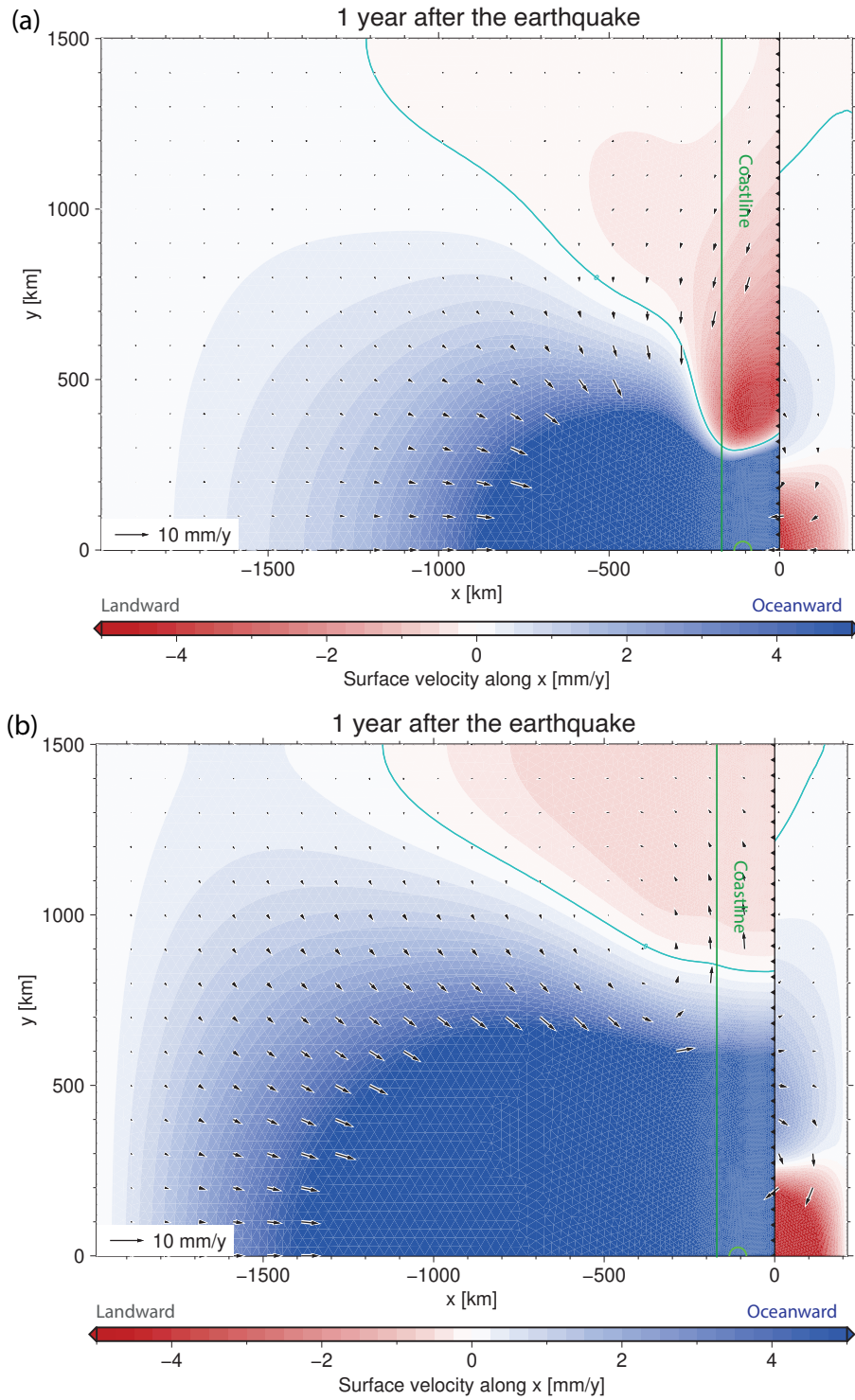


Figure S6. Trench-perpendicular velocity changes $\Delta v_{x1\text{yr-pre}}$, 1 year after the earthquake, due to viscous relaxation, in models with either (a) lower E and G and the same K as in the reference model (LoErefK), or (b) lower K and the same E (RefEloK).

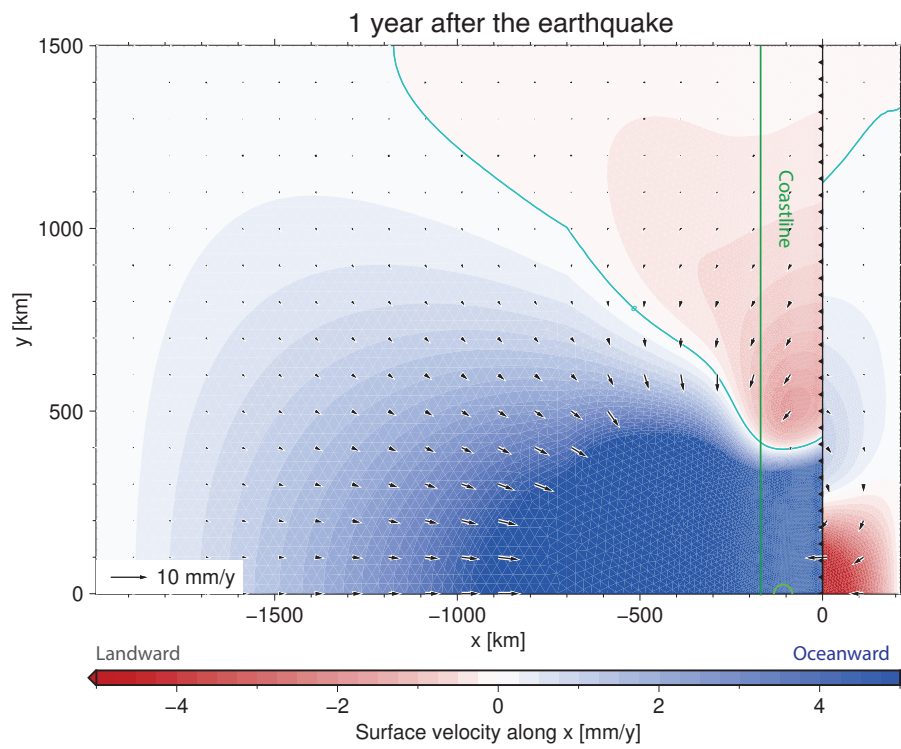


Figure S7. Trench-perpendicular velocity changes $\Delta v_{x1\text{yr-pre}}$, 1 year after the earthquake, due to viscous relaxation, in a model (E30-150) with an overriding plate E of 30 GPa at distances from the trench smaller than 700 km and 150 GPa at greater distances.

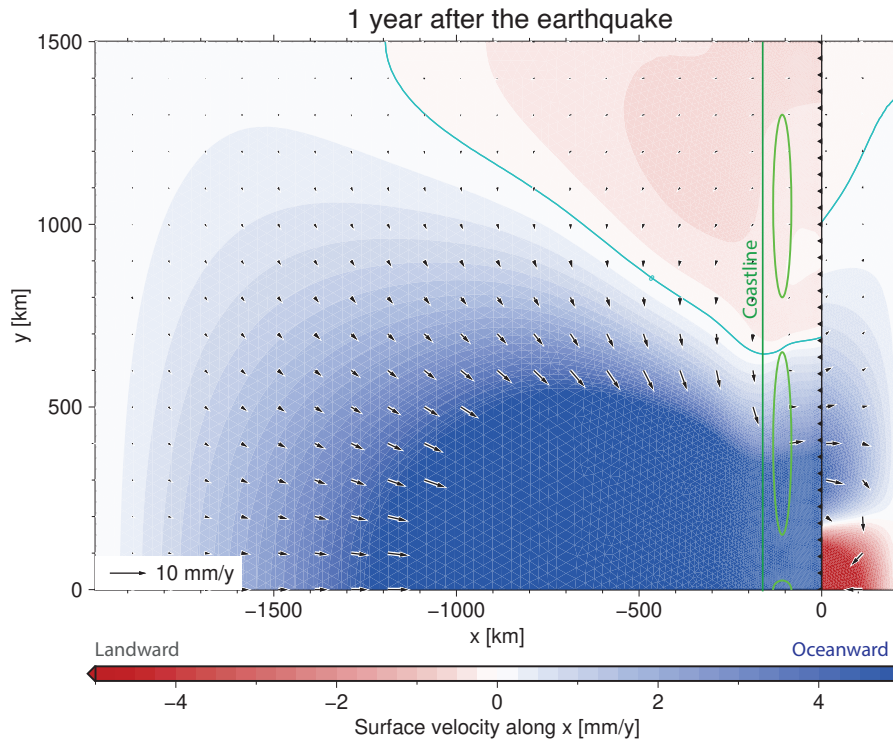


Figure S8. Trench-perpendicular velocity changes $\Delta v_{x1\text{yr-pre}}$, 1 year after the earthquake, due to viscous relaxation, in a model (LatAsp) with lateral asperities in addition to the central one (all outlined in light green), unlocked 20 (intermediate asperities) and 40 years (external asperities) after the central one.